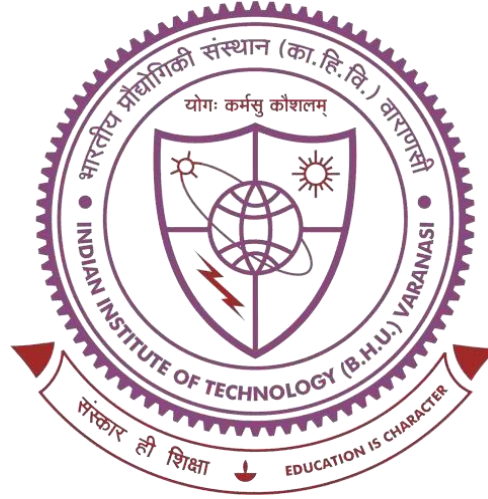


Structure and Multifunctional Properties of Hafnium Oxide Nanoparticles and Thin Films for Sensing and Resistive Switching Performance



Thesis submitted in partial fulfilment for the
award of degree

DOCTOR OF PHILOSOPHY

By

Taranga Dehury

SCHOOL OF MATERIALS SCIENCE AND TECHNOLOGY
INDIAN INSTITUTE OF TECHNOLOGY
(BANARAS HINDU UNIVERSITY)
VARANASI- 221005
INDIA

Roll No: 18111012

2024

Dedicated
to my adored Mother

CERTIFICATE

It is certified that the work contained in the thesis titled “**STRUCTURE AND MULTIFUNCTIONAL PROPERTIES OF HAFNIUM OXIDE NANOPARTICLES AND THIN FILMS FOR SENSING AND RESISTIVE SWITCHING PERFORMANCE**” by “**TARANGA DEHURY**” has been carried out under my supervision and that this work has not been submitted elsewhere for a degree.

It is further certified that the student has fulfilled all the requirements of Comprehensive, Candidacy and SOTA for the award of Ph.D. degree.

Date: 30 May 2024

Place: Varanasi

Chandana Rath

**Prof. (Mrs.) Chandana Rath
(Supervisor)**

Professor/आचार्य
School of Materials Science & Technology/पदार्थ विज्ञान एवं प्रौद्योगिकी स्कूल
Indian Institute of Technology/भारतीय प्रौद्योगिकी संस्थान
(Banaras Hindu University), Varanasi/काशी हिन्दू विश्वविद्यालय, वाराणसी

DECLARATION BY THE CANDIDATE

I, **TARANGA DEHURY**, certify that the work embodied in this Ph.D. thesis is my own bonafide work carried out by me under the supervision of **Prof. (Mrs.) CHANDANA RATH** for a period from **July 2018** to **May 2024** at the **SCHOOL OF MATERIALS SCIENCE AND TECHNOLOGY**, Indian Institute of Technology (Banaras Hindu University), Varanasi, India. The matter embodied in this Ph.D. thesis has not been submitted for the award of any other degree/diploma. I declare that I have faithfully acknowledged and given credits to the research workers wherever their works have been cited in my work in this thesis. I further declare that I have not willfully copied any other's work, paragraphs, text, data, results, *etc.*, reported in journals, books, magazines, reports, dissertations, thesis, *etc.*, or available at websites and have not included them in this thesis and have not cited as my own work.

Date. 30 May 2024

Place: Varanasi

Taranga Dehury
(Taranga Dehury)

CERTIFICATE BY THE SUPERVISOR

This is to certify that the above statement made by the candidate is correct to the best of my knowledge.

Chandana Rath

Prof. (Mrs.) Chandana Rath

Supervisor

Professor/आचार्य

School of Materials Science & Technology/पदार्थ विज्ञान एवं प्रौद्योगिकी स्कूल
Indian Institute of Technology/भारतीय प्रौद्योगिकी संस्थान
(Banaras Hindu University), Varanasi/काशी हिन्दू विश्वविद्यालय, वाराणसी

Akhilesh Singh

Prof. Akhilesh Kumar Singh

Coordinator

Coordinator/समन्वयक
School of Materials Science & Technology/पदार्थ विज्ञान एवं प्रौद्योगिकी स्कूल
Indian Institute of Technology/भारतीय प्रौद्योगिकी संस्थान
(Banaras Hindu University), Varanasi/काशी हिन्दू विश्वविद्यालय, वाराणसी

COPYRIGHT TRANSFER CERTIFICATE

Title of the Thesis: “*STRUCTURE AND MULTIFUNCTIONAL PROPERTIES OF HAFNIUM OXIDE NANOPARTICLES AND THIN FILMS FOR SENSING AND RESISTIVE SWITCHING PERFORMANCE*”

Candidate's Name: Mr. TARANGA DEHURY

Copyright Transfer

The undersigned hereby assigns to the Indian Institute of Technology (Banaras Hindu University), Varanasi all rights under copyright that may exist in and for the above thesis submitted for the award of the *Doctor of Philosophy*.

Date: 30 May 2024

Place: Varanasi

Taranga Dehury
(Taranga Dehury)

Note: However, the author may reproduce or authorize others to reproduce materials extracted verbatim from the thesis or derivative of the thesis for author's personal use provided that the source and the Institute's copyright notice is indicated.

Acknowledgements

As I reflect on my Ph.D. journey, I am filled with immense pleasure to acknowledge those who have directly or indirectly supported me during my work and stay at IIT (BHU). Expressing my heartfelt gratitude is not only a moral duty but also an act of pleasure and humility.

*First and foremost, I wish to express my sincere gratitude to my supervisor, **Prof. (Mrs.) Chandana Rath**, for her trust, nice guidance, faithful support and valuable suggestions throughout my Ph.D. work. Her constant monitoring and interest in my work will always remain as a happy memory. Her patient and enthusiastic approach to my training cannot be expressed in words and I will always be thankful to her.*

I would also like to express my sincere thanks to Prof. Suranjan Panigrahi (host Professor at Purdue University during SERB overseas visiting doctoral fellowship), for his constant guidance, valuable suggestions, encouragement and support. I am very grateful to my RPEC members Prof. Akhilesh Kumar Singh, School of Materials Science & Technology, IIT (BHU) and Dr. Shail Upadhyay, Department of Physics, IIT (BHU), for their stimulating help and criticism which incited me to widen my research from various perspectives. I would like to thank the coordinator of School of Materials Science and Technology, IIT (BHU) for providing different instrumental facility. I would like to convey my gratitude to Dr. Ravi Panwar (DPGC convener) for his valuable inputs, suggestions and affectionate attitude.

I wish to express deep regards to all the professors of the School, Prof. D. Pandey, Prof. R. Prakash, Prof. P. Maiti, Dr. C. Upadhyay, Dr. B. N. Pal, Dr. Sanjay Singh, Dr. A. K. Mishra, Dr. S. K. Mishra, Dr. N. Kumar, Dr. U. Shankar, Dr. A. Kumar and others for their kind support at all moment during the progress of my research.

With a deep sense of gratitude, I convey my sincere thanks to CIFC, IIT (BHU), Varanasi for help in carrying out characterizations of the synthesized samples. I would like to greatly acknowledge our collaborators, Prof. ASK Sinha, Dr. Mukul Gupta, Dr. Sabine Pütter and Dr. Satyaprakash Sahoo, for their help in different projects. I am also grateful to all office staff of the School of Materials Science and Technology and authorities of IIT (BHU), for their kind help during the period of my stay to complete the thesis work.

My sincere gratitude to dear seniors and colleagues of our lab: Dr. Pankaj Mohanty, Dr. Vinay Pratap Singh, Dr. Himanshu Tripathy, Dr. Jagdish Kumar G, Dr. Durgesh Kumar, Dr. B. Bharti, Dr. Sandeep Kumar, Dr. Priyanka Tiwari, Dr. Deepti Gangwar, Mr. Manish Yadav, Dr. Abhay Narayan Singh, Mr. Akhilesh Yadav, Ms. Sanjana Rajput, Mr. Keshav Kumar, Ms. Aiswarjya Bastia, Mr. Deepankar Das, Ms. Leskhmi S Kumar. I am extremely thankful to my dear friends Dr. Rajnikant, Dr. Raman, Pawan, Krishnakant, Dr. Vivek, Rohit Kumar, Rohit Ranjan, Krishan Kumar, Soumya, Sagar, Divya, Dr. Arun, Dr. Akash, Nihar, Biswajit, Dr. Pankaj, Dr. Kalpana and Heiner for their unconditional cooperation and sincere help in every possible way as well as for making this journey an enjoyable one.

It fills me with a deep sense of reverence when I think of my family, especially my Father Sh. Sriram Dehury, Mother Late Smt. Suryamani Behera and younger Brother Mr. Rajat Dehury. Their constant encouragement, moral support and cooperation at every step of my life cannot be expressed in words. I am extremely thankful for their love and blessings.

Finally, I bow with reverence and gratitude to thank the Almighty Lord SHREE JAGANNATH, Lord KASHI VISHWANATH and Goddess DURGA, who have enriched me with such an excellent opportunity and infused the power in my mind to fulfill the work assigned to me.

Date: 29 May 2024

Place: Varanasi

Taranga Dehury

(Taranga Dehury)

Contents

<i>Acknowledgements</i>	vii
<i>Contents</i>	ix
<i>List of Figures</i>	xiii
<i>List of Tables</i>	xvii
<i>Abbreviations and Symbols</i>	xix
PREFACE	xxiii
Chapter 1 Introduction and Literature Review	1
1.1 Introduction.....	1
1.1.1 Transition Metal Oxides.....	1
1.1.2 HfO ₂ and its Crystal Structure.....	2
1.1.3 Physical and Chemical Properties of HfO ₂	5
1.2 Literature Review.....	7
1.2.1 Green Synthesis.....	7
1.2.2 Structural Transformation in HfO ₂ : Effect of Synthesis Parameters and Dopants.....	9
1.2.3 HfO ₂ Nanostructures for Sensor Application.....	14
1.2.4 HfO ₂ Nanostructures for Memory Device Application.....	17
1.3 Objectives.....	23
Chapter 2 Experimental Methods	27
2.1 Introduction.....	27
2.2 Synthesis of Nanoparticles.....	28
2.2.1 Sol-gel Technique.....	28
2.2.2 Green Synthesis Method.....	29
2.3 Deposition of Thin Films.....	30

2.3.1	Ion Beam Sputtering (IBS)	30
2.3.2	Molecular Beam Epitaxy (MBE).....	32
2.4	Fabrication of Memory Device	33
2.5	Characterization Techniques	34
2.5.1	X-ray Diffraction (XRD)	34
2.5.2	Grazing Incidence X-ray Diffraction (GIXRD).....	36
2.5.3	X-ray Reflectivity (XRR)	37
2.5.4	Raman Spectroscopy.....	37
2.5.5	Fourier Transform Infrared Spectroscopy (FTIR)	38
2.5.6	Transmission Electron Microscopy (TEM)	39
2.5.7	Atomic Force Microscopy (AFM).....	40
2.5.8	X-ray Photoelectron Spectroscopy (XPS)	41
2.5.9	Auger Electron Spectroscopy (AES)	42
2.5.10	UV-visible Spectroscopy	43
2.5.11	Electrochemical Impedance Spectroscopy (EIS).....	44
2.5.12	Polarization Measurements: <i>P-V</i> Hysteresis Loop Tracer	45
2.5.13	Electrical Measurements: <i>I-V</i> , Endurance and Retention	46
Chapter 3 Structural Transformation and Bandgap Engineering by Doping Pr in Nanoparticles of HfO₂.....		49
3.1	Introduction	49
3.2	Structure, Microstructure and Phase Transformation	49
3.2.1	XRD, Raman Spectroscopy and FTIR Spectroscopy	49
3.2.2	Microstructural Analysis.....	56
3.2.3	X-ray Photoelectron Spectroscopy	57
3.2.4	Mechanism for Phase Transformation from Monoclinic to Cubic	59
3.3	Optical Properties: Bandgap Estimation	61
3.4	Conclusions	63

Chapter 4 Green Synthesis of HfO₂ Nanoparticles for their Sensing Application .65	
4.1 Introduction.....	65
4.2 Green Synthesis and Characterizations.....	65
4.2.1 Green Synthesis and Mechanism.....	65
4.2.2 Structure, Microstructure and Optical Properties.....	67
4.3 Liquid Ammonia Sensing using Electrochemical Impedance Spectroscopy... 71	
4.4 Conclusions.....	74
Chapter 5 Thickness Dependent Phase Transformation and Resistive Switching Performance of HfO₂ Thin Films Fabricated by Ion Beam Sputtering.....75	
5.1 Introduction.....	75
5.2 Structure and Microstructure.....	76
5.2.1 Thickness, Density and Roughness by X-ray Reflectivity.....	76
5.2.2 Surface Morphology by Atomic Force Microscopy.....	76
5.2.3 Structure and Phase Transformation.....	79
5.2.4 X-ray Photoelectron Spectroscopy and UV-visible Spectroscopy.....	80
5.3 Resistive Switching Behavior.....	83
5.3.1 Current-Voltage (<i>I-V</i>) Characteristics.....	83
5.3.2 Endurance and Retention Measurements.....	87
5.3.3 Mechanism for Resistive Switching.....	87
5.4 Conclusions.....	92
Chapter 6 Structure and Resistive Switching Behavior of Molecular Beam Epitaxy Grown HfO₂ Thin Films.....95	
6.1 Introduction.....	95
6.2 Structure and Microstructure.....	95
6.2.1 Structure through Grazing Incidence X-ray Diffraction.....	95
6.2.2 Thickness, Density and Roughness by X-ray Reflectivity.....	97
6.2.3 Surface Morphology by Atomic Force Microscopy.....	98
6.2.4 Auger Electron and X-ray Photoelectron Spectroscopy.....	99

6.3	Resistive Switching Behavior	101
6.3.1	Current-Voltage (I - V) Characteristics	101
6.3.2	Mechanism for Resistive Switching	103
6.4	Conclusions	106
Chapter 7 Summary and Future Scope		107
7.1	Summary	107
7.2	Future Scope.....	109
<i>References</i>		111
<i>List of Publications</i>		127

List of Figures

Figure 1.1 Three crystal phases of HfO ₂ as a function of temperature under ambient pressure.....	3
Figure 1.2 Phase diagram of Temperature vs. Pressure HfO ₂	5
Figure 1.3 Different applications of HfO ₂ nanostructures in various industries.....	6
Figure 1.4 X-ray diffraction patterns indicating stabilization of the monoclinic and tetragonal phase in stoichiometric and oxygen deficient HfO ₂ films.	11
Figure 1.5 X-ray diffraction data of (a) cubic and (b) monoclinic HfO ₂ nanoparticles. Selected area electron diffraction (SAED) patterns of respective phases are displayed in the insets.	12
Figure 1.6 A typical current-voltage (I-V) diagram depicting different processes of resistive switching.....	18
Figure 2.1 Flow chart of sol-gel technique for the synthesis of pure HfO ₂ and Pr doped HfO ₂ nanopowders.....	28
Figure 2.2 Schematic diagram of HfO ₂ synthesis from orange peel extracts via green sol-gel route.	30
Figure 2.3 A schematic representation of meta-insulator-metal (MIM) structure.	34
Figure 2.4 A schematic diagram of incident and diffracted X-rays from equidistance lattice planes in the crystal.	35
Figure 2.5 (a) General set-up for 3 electrodes configuration and (b) schematic diagram of our connection of the screen-printed electrode to the Gamry Reference 600 potentiostat (diagram is not to scale).	45
Figure 2.6 Schematic representation of Sawyer tower circuit for ferroelectric hysteresis measurements.....	46
Figure 2.7 Schematic diagram of the circuit connection of HfO ₂ based memristor.....	47
Figure 3.1 X-ray diffraction patterns of Hf _{1-x} Pr _x O ₂ (0 ≤ x ≤ 0.15) nanoparticles calcined at 900 °C for 5 hours.	50
Figure 3.2 Phase fraction of the cubic phase as a function of Pr concentration.....	51
Figure 3.3 Rietveld refinement of the XRD patterns using FullProf software.....	52

Figure 3.4 Variation in crystallite size and lattice strain of $Hf_{1-x}Pr_xO_2$ ($x = 0-0.15$) nanoparticles.....	53
Figure 3.5 Raman modes monoclinic ($x = 0$) and cubic ($x = 0.15$) phase of $Hf_{1-x}Pr_xO_2$ nanoparticles.....	54
Figure 3.6 Transmittance spectra of $Hf_{1-x}Pr_xO_2$ nanoparticles ($x = 0, 0.01, 0.09$ and 0.15) from Fourier transform infrared spectroscopy.....	55
Figure 3.7 SAED patterns and high-resolution TEM for (a, b) $x=0$ and (c, d) $x=0.15$; TEM micrographs and the particle size distribution histograms are shown as the insets of (a) and (c) for respective sample.....	57
Figure 3.8 (a), (b), (c) XPS spectra of O 1s and (d), (e) Pr 3d core levels of $Hf_{1-x}Pr_xO_2$ nanoparticles.....	58
Figure 3.9 Pr 3d core level spectra of $Hf_{1-x}Pr_xO_2$ ($x = 0, 0.09$ and $x = 0.15$) nanoparticles.....	59
Figure 3.10 UV-visible absorption spectra of $Hf_{1-x}Pr_xO_2$ ($x = 0, 0.09$ and 0.15) nanoparticles.....	62
Figure 3.11 Tauc plots of $Hf_{1-x}Pr_xO_2$ nanoparticles (a) $x = 0$, (b) $x = 0.09$ and (c) $x = 0.15$	62
Figure 4.1 Chemical mechanism of green synthesis of HfO_2 nanoparticles using orange peel extracts.....	67
Figure 4.2 XRD patterns of green synthesized HfO_2 nanoparticles (HO-1-OPE, HO-2-OPE and HO-4-OPE).....	68
Figure 4.3 Transmission electron micrographs of (a) HO-1-OPE, (b) HO-2-OPE and (c) HO-4-OPE.....	68
Figure 4.4 (a) Le Bail profile fitting, (b) Williamson-Hall plot of HfO_2 sample and (c) average particle size histogram of HO-4-OPE.....	69
Figure 4.5 UV-visible absorbance spectra of HO-1-OPE, HO-2-OPE and HO-4-OPE.....	70
Figure 4.6 Bode plots obtained from EIS measurements at different liquid ammonia concentrations with 10 mV ac voltage in 100 mHz to 1 MHz frequency range. Inset represents the model used for the fitting.....	72
Figure 4.7 Nyquist plots obtained from EIS measurements at different liquid ammonia concentrations with 10 mV ac voltage in 100 mHz to 1 MHz frequency range.....	73

Figure 4.8 (a) Variation of charge transfer resistance with respect to ammonia concentrations and (b) prediction model to predict ammonia concentration of real samples.....	74
Figure 5.1 X-ray reflectivity spectra of HfO ₂ thin films having thicknesses of ~ 10, 20 and 30 nm. Insets show the schematic diagram of the stacking used for fitting the XRR spectra (diagrams are not to scale).	77
Figure 5.2 AFM analysis of the fabricated HfO ₂ thin films of ~ 10, 20 and 30 nm thickness. The film roughness is found to be 0.3, 0.6 and 0.6 nm for 10, 20 and 30 nm films, respectively.....	78
Figure 5.3 GIXRD data for HfO ₂ thin films with ~ 10, 20 and 30 nm thickness [<i>m</i> = monoclinic (P21/c), <i>o</i> = orthorhombic (Pbca) phase].	80
Figure 5.4 (a, b) Hf 4f and (c, d) O 1s core level XPS spectra of oxygen deficient HfO ₂ thin films having thicknesses of ~ 20 and 30 nm.	81
Figure 5.5 (a) Absorbance spectra and (b) band gap of HfO ₂ thin films with thicknesses of ~ 20 and 30 nm.	83
Figure 5.6 Current-voltage (I-V) characteristics in semilogarithmic scale for RRAM devices based on HfO ₂ films of ~ 10, 20 and 30 nm thickness.	85
Figure 5.7 SET and RESET voltage distribution of five RRAM devices based on HfO ₂ film of 20 nm thickness.....	86
Figure 5.8 Current-voltage (I-V) characteristics in semilogarithmic scale for RRAM devices based on HfO ₂ film of 30 nm thickness.	87
Figure 5.9 (a) The endurance and (b) the retention characteristics at a readout voltage of 1 V of RRAM devices based on HO10, HO20, and HO30. The double-sided arrow indicates the storage window of the RRAM device based on HO20.....	88
Figure 5.10 (a) Ohmic and (b) Poole-Frenkel model linear fits for LRS and HRS, respectively, for 20 nm HfO ₂ film (Ohmic model is shown in log-log scale).	89
Figure 5.11 P-V loops obtained from hysteresis measurements of HfO ₂ thin film of 20 nm thickness (HO20).	91
Figure 5.12 Resistive switching mechanism in oxygen deficient of HfO ₂ thin films (TE- top electrode, BE- bottom electrode, LRS- low resistance state, HRS- high resistance state).....	92
Figure 6.1 GIXRD patterns for HfO ₂ thin films deposited at substrate temperature of 300 (Film A) and 500 °C (Film B) along with the standard JCPDS data.	96

Figure 6.2 (a,b) X-ray reflectivity spectra for film A and Film B and (c) schematic diagram of the stacking model.....	97
Figure 6.3 2D and 3D AFM micrographs of the Film A and Film B.....	98
Figure 6.4 Auger electron spectra of the HfO ₂ films.....	99
Figure 6.5 (a,b) Hf 4f and (c,d) O 1s core level XPS spectra of Film A and Film B... ..	100
Figure 6.6 (a) Schematic diagram, (b) device-to-device variation and (c) 1 st , 50 th and 100 th I-V cycles of the memristor based on Film A.....	102
Figure 6.7 (a) Schematic diagram, (b) device-to-device variation and (c) 1 st , 50 th and 100 th I-V cycles of the memristor based on Film B.....	102
Figure 6.8 I-V characteristics for Film B in the applied voltage range of 0 V → -5 V → 0 V → 5 V → 0 V.....	103
Figure 6.9 Resistive switching mechanism for volatile memristor.....	105

List of Tables

Table 1.1 List of green synthesis of metal oxide nanoparticles with used green source and remarks on the applications of green nanomaterials. 9

Table 1.2 A brief list of reports for optimizing resistive switching performance using filament control..... 21

Table 3.1 Optimized cell parameters and cell volume for $Hf_{1-x}Pr_xO_2$ ($x = 0$ and $x = 0.15$) compared with standard JCPDS data for monoclinic and cubic phase of HfO_2 52

Abbreviations and Symbols

Abbreviations

AFM	Atomic force microscope
AI	Artificial intelligence
at%	Atomic percentage
BE	Binding energy
CFs	Conductive filaments
CIFC	Central instrument facility center
CMOS	Complementary metal oxide semiconductor
DI	Deionized
EG	Ethylene glycol
EIS	Electrochemical impedance spectroscopy
eV	Electron volt
Exp.	Experimental
GIXRD	Grazing incidence X-ray diffraction
GPa	Giga Pascal
HRS	High resistance state
HRTEM	High resolution transmission electron microscopy
IDLH	Immediately dangerous to life or health
$I-V$	Current voltage
JCPDS	Joint committee on powder diffraction standards
KE	Kinetic energy
keV	Kilo electron volt
kHz	Kilo Hertz

kV	Kilo volt
LRS	Low resistance state
μ A	Micro ampere
mA	Milli ampere
mg	Milligram
MIM	Metal-insulator-metal
ML	Machine learning
μ L	Microliter
μ m	Micrometer
mm	Millimeter
NIOSH	National institute for occupational safety and health
nm	Nanometer
NMP	N-methyl pyrrolidone
No.	Number
NVS	Nonvolatile switching
OPE	Orange peel extract
OSHA	Occupational safety and health administration
PPF	Pair pulse facilitation
ppm	parts per million
p^{++} -Si	Heavily doped p-type silicon
<i>P-V</i>	Polarization voltage
PVDF	Polyvinylidene fluoride
RE	Rare earth
RRAM	Resistive random access memory
RT	Room temperature

SAED	Selected area electron diffraction
STDP	Spike time-dependent plasticity
STM	Short-term memory
TEM	Transmission electron microscopy
TMO	Transition metal oxides
TWA	Time weighted average
UV	Ultra violet
vs.	Versus
VS	Volatile switching
wt%	Weight percentage
XPS	X-ray photo electron spectroscopy
XRD	X-ray diffraction

Symbols

Å	Angstrom
°C	Degree Centigrade
d	Interplanar spacing
h	hour
k	Dielectric constant
K	Kelvin
λ	Wavelength
P	Pressure
T	Temperature
V_o	Oxygen vacancy
V_o^+	Singly charged oxygen vacancy
V_o^{++}	Doubly charged oxygen vacancy

PREFACE

Nanostructured binary transition metal oxides (TMOs) are technologically important class of smart materials that possess high interest because of their great chemical stability, simple structure and low-cost production. These functional materials are considered to be the building blocks of next-generation advanced electronic devices. Different TMOs such as TiO₂, VO₂, MnO₂, Fe₂O₃, NiO, ZnO, WO₃, ZrO₂ and HfO₂, having diverse morphology and dimensions, are now being explored for their implementation in a wide range of applications such as photocatalysis, transparent semiconductor devices, spintronics, sensing of toxic compounds, scintillation, optoelectronics, energy storage, fuel cells, memory devices etc. Among all TMOs, hafnium oxide (HfO₂) has been consistently researched as a prospective material, mainly as an alternative to silicon for the semiconductor industry. Because of its appropriate high-*k* value and high thermal stability against silicon, HfO₂ is proven to be a potential candidate for gate dielectric material in metal oxide field effect transistors (MOSFETs). Since 2007, HfO₂ has been used as the gate dielectric in Intel's 45 nm quad-core processor, replacing SiO₂. Moreover, HfO₂ finds promising applications in anti-reflection coatings, X-ray phosphors, gas/liquid sensing, latent fingerprint imaging, cellular imaging, ferroelectric and resistive switching memory devices, etc. At room temperature, bulk HfO₂ crystallizes into a monoclinic phase, transforming to tetragonal and cubic phases at 1700 °C and 2600 °C, respectively. Reported literature indicates that the high temperature tetragonal and cubic phases of HfO₂ exhibit high dielectric constant (*k*) of approximately 70 and 25, respectively. First principle calculations suggest that these high temperature phases can be stabilized at room temperature by doping with elements of lower valency. Various authors have explored the impact of trivalent element doping, with ionic radii different from that of Hf, on the stability of the tetragonal and cubic phases of HfO₂. It has been

found that dopants with smaller ionic radii, such as Si, Ge, Sn, P, Al or Ti stabilize the tetragonal phase, while those with larger ionic radii, such as Y, Gd, Sc, Dy or Sm stabilize the cubic phase at room temperature.

HfO₂ nanostructures are usually insulators with an ionic conduction where oxygen ions are the primary mobile species. However, impurities, crystallographic defects and especially oxygen vacancies created during synthesis can introduce intermediate states in the band gap region, turning it into an n-type semiconductor suitable for various technological applications. There are limited reports available in the literature on the sensing activity of HfO₂ nanostructures. Capone *et al.* and Durrani *et al.* analyzed the CO gas sensing properties of the HfO₂ thin films. HfO₂ based nanostructures are also investigated for their sensitivity toward hydrogen, propane and humidity. Besides, HfO₂ has garnered significant attention for its potential applications in next-generation data storage devices. Resistive switching based memory devices operate by switching between low and high resistive states under an applied bias voltage. In this context, stable, uniform and reproducible bipolar resistive switching in HfO₂ based memory devices has been reported by Jančovič *et al.*, Hua *et al.* and Kumar *et al.*

The synthesis of HfO₂ plays a crucial role in optimizing the performance of nanostructured devices by desirably tuning the required parameters. Nowadays, green synthesis is gaining popularity over conventional synthesis methods as it is environment-friendly and cost-effective for large-scale production. Advanced thin film deposition techniques, such as atomic layer deposition (ALD), pulsed laser deposition (PLD), ion beam sputtering (IBS) and molecular beam epitaxy (MBE), are used to have firm control over HfO₂ film thickness, density, surface roughness, etc., which play a pivotal role in determining the performance, stability and endurance of the device.

In this work, we aim to provide a comprehensive exploration of nanostructured HfO₂, focusing on both structural characteristics and multifunctional attributes. The study is motivated by the potential applications of HfO₂ in advanced sensing technologies and resistive switching devices, making it particularly relevant in the context of emerging electronics and memory technologies. The primary objectives of this study include investigating the morphological intricacies of HfO₂ nanoparticles and thin films, examining their crystalline structure and evaluating their multifunctional properties, particularly in the realms of sensing applications and resistive switching performance.

Organization of Thesis

The thesis is organized into **Seven Chapters** as follows.

Chapter 1 provides a concise overview of the structural, microstructural, physical and chemical properties of HfO₂ nanostructures, along with a brief literature survey on the green synthesis methods. Our investigation extends to various applications of HfO₂ nanoparticles and thin films, such as optical devices, toxic compound sensors and resistive switching memory devices. This chapter shows the noteworthy outcomes of the research, summarizing the key contributions in this field. Based on the literature survey, the objective of the thesis is outlined and accordingly, the results, discussions and important findings are presented in four different chapters.

In **Chapter 2**, we present a summary of the methodologies utilized for the synthesis of HfO₂ nanoparticles, such as sol-gel and green synthesis methods, along with the fabrication of HfO₂ thin films using ion beam sputtering and molecular beam epitaxy. The chapter also addresses characterization techniques that are used for data collection and calibration. The structural and microstructural analysis is carried out using X-ray diffractometer, X-ray reflectometer, Raman spectrometer, FTIR spectrometer, TEM

AFM, XPS and AES. Absorbance spectra and optical band gap are examined using UV-visible spectrophotometer. Sensing performance is evaluated through a potentiostat through electrochemical impedance spectroscopy. A ferroelectric loop tracer is used for P - V hysteresis measurements. For electrical measurements, such as I - V cycles, retention and endurance measurements, etc., a semiconductor parameter analyzer is utilized.

Chapter 3 discusses the stabilization of the high-temperature cubic phase of HfO_2 at room temperature by doping Pr up to 15 at%. While the monoclinic phase remains stable below 7 at%, the coexistence of monoclinic and cubic phases is observed between 7 and 13 at% of Pr. With doping, the average particle size is reduced from 35 to 10 nm, accompanied by enhanced strain estimated from Williamson-Hall plots. The optical bandgap decreases from 5.42 eV in pure HfO_2 to 5.06 eV in 15 at% Pr doped HfO_2 due to non-stoichiometry and formation of sub-bands near the conduction band. Such exciting results are discussed on the basis of enhanced oxygen vacancies inducing 8-fold oxygen coordinated Pr^{3+} ions in the lattice that stabilize the cubic phase of HfO_2 .

In **Chapter 4**, we have synthesized HfO_2 nanoparticles via green route using orange peel extracts (1, 2 and 4 wt%). HfO_2 nanoparticles synthesized with 4 wt% orange peel extract and calcined at 900 °C for 1 h (HO-4-OPE) show well dispersed nanoparticles of size 34 nm with maximum yield. A sensing framework to detect liquid NH_3 is developed using HfO_2 nanoparticle coated electrode and electrochemical impedance spectroscopy. We have successfully detected liquid NH_3 of concentrations 50 to 500 ppm with charge transfer resistance as the sensing parameter. An exponential relation between charge transfer resistance and NH_3 concentration is observed. Here, for the first time, we have used the green synthesis technique to synthesize HfO_2 nanoparticles for the liquid NH_3 sensing application.

In **Chapter 5**, we demonstrate the performance of RRAM devices using HfO₂ thin films deposited using the ion beam sputtering technique on p⁺⁺-Si (100) substrate by varying thickness from 10 to 30 nm with density in the range of 9.1-8.6 g/cm³. A drastic change in the average grain size from ~ 90 to ~ 2000 nm is noticed along with a structural transformation from orthorhombic to dominant monoclinic phase when the thickness is increased from 20 to 30 nm. The phase transformation is accompanied by a significant increase in the average grain size along with a decrease in the oxygen vacancy. Further, a red shift in the absorption peak and a reduced band gap of HfO₂ film having 30 nm thickness well corroborates with the above fact. Among all films, the film of 20 nm thickness shows better switching behavior with an ON/OFF ratio of ~ 7, attributed to the appropriate grain size, enhanced crystallization, and oxygen vacancies. The ON/OFF ratio observed here is higher than that of monoclinic (~ 3), tetragonal (~ 5) and cubic (~ 3) phases, reported earlier. The endurance and retention measurements show the excellent reliability of the 20 nm thick device. Schematically, the switching mechanism has been discussed based on the Ohmic and Poole-Frenkel conduction models, which is attributed to the formation and rupture of conductive filaments consisting of oxygen vacancies.

Chapter 6 describes the structure, morphology and resistive switching aspects of molecular beam epitaxy grown HfO₂ thin films fabricated on p⁺⁺-Si (100) substrate at substrate temperature of 300 and 500 °C. The crystalline nature and monoclinic phase (*P2₁/c*) of the HfO₂ films are confirmed by the GIXRD patterns. The density of the HfO₂ layer is found to be 9.1 and 9.2 g/cm³, whereas the root mean square roughness is found to be 1.34 and 2.40 nm with average grain size of 140 nm in the films with substrate temperature of 300 and 500 °C, respectively. Both films demonstrate forming free volatile resistive switching behavior with SET voltage of -3.1 and -3.6 V, along with the ON/OFF ratio of ~ 2 and ~ 4 for the films with substrate temperature of 300 and 500 °C,

respectively. Memory device based on HfO₂ film with higher substrate temperature exhibits a better ON/OFF ratio due to higher crystallinity and availability of more oxygen vacancies. A comprehensive mechanism of resistive switching is also discussed in this chapter, considering the transport of Ag ions and oxygen vacancies.

In Chapter 7, we have summarized the important findings of this thesis work, along with a discussion of the future prospects. We have been working on the structure and multifunctional properties of nanostructured HfO₂ for sensing and resistive switching applications. We would like to extend our work into application-oriented domains such as optoelectronic devices using HfO₂ nanoparticles. Resistive switching performance of HfO₂ based memory devices could be optimized and explored for neuromorphic computing applications.

A list of journals and books used to bind up the thesis has been given at the end as references.